Diffusion Foundations
ISSN: 2296-3642, Vol. 26, pp 63-77

Submitted: 2019-10-01
Accepted: 2019-10-16
Online: 2020-03-02

Convective Heat Transfer Analysis of Hydromagnetic Micropolar Fluid Flow Past an Inclined Nonlinear Stretching Sheet with Variable Thermo-Physical Properties

Ephesus Olusoji Fatunmbi[1], Samuel Segun Okoya[2], Oluwole Daniel Makinde[3]

[1]Department of Mathematics and Statistics, Federal Polytechnic, Ilaro, Nigeria.

[2]Department of Mathematics, Obafemi Awolowo University, Ile-Ife, Nigeria

[3] Faculty of Military Science, Stellenbosch University, Private Bag X2, Saldanha 7395, South Africa.

[1]olusojiephesus@yahoo.com, [2]ssokoya@gmail.com, [3]makinded@gmail.com

Keywords: Convective heating; micropolar fluid; nonlinear stretching sheet; variable properties

Abstract The current work examines mixed convection boundary layer flow and heat transfer attributes in hydromagnetic micropolar fluid past a heated inclined sheet which stretches nonlinearly along the direction of flow. The impact of variable thermo-physical characteristics of the fluid together with the influence of magnetic field, thermal radiation and viscous dissipation are also checked on the flow field. The modelled governing equations are translated from partial to ordinary differential equations via relevant similarity transformations and the resulting equations are subsequently solved numerically by means of shooting techniques in company with Runge-Kutta integration algorithms. The reactions of the skin friction coefficient, Nusselt number, dimensionless velocity as well as temperature to variations in the emerging controlling parameters are illustrated through different graphs. In the limiting situations, the results obtained exhibit a strong relationship with the existing related works in literature. The facts emanated from this study also reveal that the thickness of the thermal boundary layer grows widely with a rise in the Eckert number and Biot number parameters whereas increasing the material (micropolar) and thermal conductivity parameters have opposite effects on the rate of heat transfer.

Introduction

Studies have shown that the Newtonian fluid models are incapable of describing accurately the characteristics of complex and complicated fluids such as fluids with microstructures and suspended particles which are encountered in various areas of engineering, science and technology [1-2]. This has necessitated and compel researchers and scientists to pay more attention to the study of non-Newtonian fluids flow which has significant applications both in engineering and industrial processes such as in food processing and cosmetics industries, oil drilling, chemical engineering, paints rheology, fluid suspension and additives, molten polymers, etc. Notable among the non-Newtonian fluid models which has been found suitable to effectively describe, model and simulate various complex and complicated fluids with rigid molecules, bar-like particles and microstructure is the concept of micropolar fluid initiated by [3-4]. The flow equations of micropolar fluid are characterized by the inclusion of microrotation vector alongside with the classical velocity vector such that the field of microrotation and macro-velocity are also coupled together. Such fluids include polymeric fluids, fluid suspensions, animal blood, lubricants, liquid crystals, colloidal fluids and so on [5-7] and they are widely applicable in engineering and industrial activities including the bio-mechanic and chemical engineering, extrusion of polymer, slurry technologies, synovial lubrication, arterial blood flows, knee cap mechanics, etc. [8-10].

Fluid flow prompted by stretched sheet was instituted by [11] who investigated the problem with constant velocity. The case in which the velocity is proportional to the distance from the silt was first studied by [12]. During fabrication processes such as in polymer extrusion, the grade of the end product is determined by the rate of stretching and the rate at which the objects are cooled [13]. Such studies therefore find practical applications in industrial and engineering operations such as drawing of wires, manufacturing of paper and textile, the aerodynamic extrusion of plastic sheet, glass blowing, etc. Other investigations on various aspect of such study with the inclusion of various parameters, different geometries and boundary situations have been conducted [14-19].

When heat conduction at the surface of the material corresponds to the heat convection at the surface in the same direction then the convective boundary conditions is assumed. This type of condition offers general and realistic prediction particularly in numerous engineering and industrial works such as transpiration cooling process, heat exchangers, material drying, conjugate heat transfer around fins and so on. To this end, [20] addressed such problem over a flat impermeable plate and reported the possibility of similarity solution when the convective heat transfer is proportional to $\frac{1}{\sqrt{x}}$ while [16] studied a case with permeable plate. Also, the knowledge of thermal radiation becomes important in most engineering areas, such as fossil fuel combustion energy processes, solar power technology, gas turbines and space vehicle re-entry for building advanced energy conversion systems. In such systems, thermal radiation takes place due to the emission by the heated surface and the working fluids, high differences between the surface and ambient temperature, for instance, in polymer extrusion processing, the quality of the final product is determined to some extent on thermal controlling factors [21-23].

The above studies were carried with the condition that the thermo-physical properties of the fluid are constant in the flow field but it has been observed that these properties may be altered by the temperature changes [24-25]. The heat being generated internally as a result of fluid friction accompany with temperature variations may have significant influence on these properties and consequently the hydrodynamic and thermal boundary layers can be affected which can lead to changes in the wall heat transfer. Besides, heat from the external source in form of ambient temperature with high shear rates can enhance generation of temperature which may have great impact on the properties of the fluid and then affect the flow structure [26]. Hence, to ensure more realistic prediction, variable properties of the fluid should be accounted for in the flow field. In the light of great industrial usage of such studies as in process of wire drawing, food and polymer processing, paper and textile production, various authors [27-31] have investigated such study where the viscosity is directly or inversely related to the temperature.

In particular, the current study tends to improve on the work of [32] by investigating the effects of variable fluid properties on the flow field, the impact of the inclination, thermal radiation effect and the influence of the surface mass flux (suction/injection) on the proposed model problem. Graphical representations and numerical values are given while the results are compared with the earlier related results in literature. Good agreement are found for the comparison.

Mathematical Formulation of the Problem

The sketch of the physical model and flow configuration is described in Figure 1 where the flow is supposed to be two-dimensional over a permeable stretching sheet being inclined at angle φ to the gravity acceleration vector. Also, it is presumed that the flow is steady, laminar, incompressible, steady and viscous boundary layer flow while the fluid is hydromagnetic micropolar fluid. The sheet stretches nonlineraly with a velocity $u_w = cx^r$ with $c > 0$ being a constant, r denotes the nonlinear stretching parameter and x the coordinates taking along the stretching sheet. Neglecting the induced magnetic

and electric field and suppose that the external magnetic field of uniform strength is applied normal to the flow direction. The properties of the fluid are believed to be variable type given in Eqs. (6-8) while the temperature of the sheet is upheld by a convective heating process from a hot fluid having a temperature T_f. The impact of Joule heating as well as viscous dissipation and thermal radiation are included in the model. Use has been made of the boundary layer together with Oberbeck-Boussinesq approximations for simplification in the this model. Taking cognizance of the aforementioned assumptions, the equations of continuity, momentum, microrotation and that of energy are respectively listed as follow:

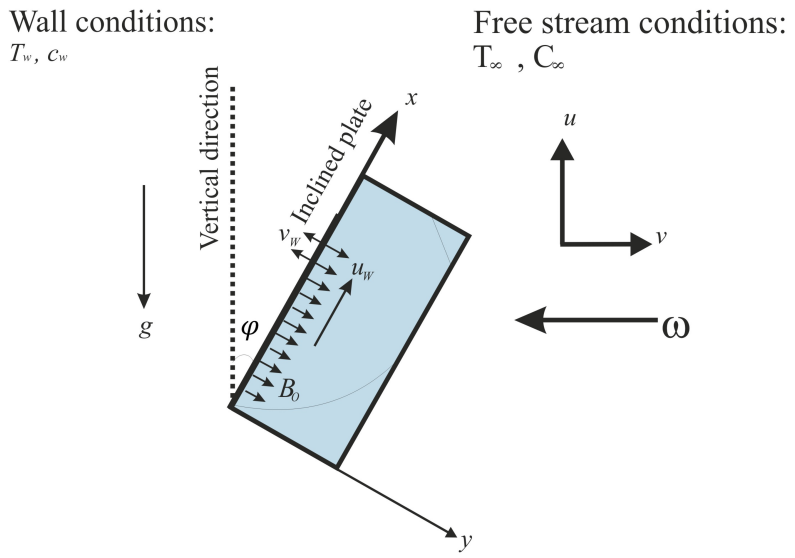

Fig. 1 The Sketch of the Physical Model

$$\frac{\partial u}{\partial x}+\frac{\partial v}{\partial y}=0, \tag{1}$$

$$u\frac{\partial u}{\partial x}+v\frac{\partial u}{\partial y}=\frac{1}{\rho_\infty}\left[\frac{\partial}{\partial y}\left(\mu(T)\frac{\partial u}{\partial y}\right)+\mu_r\frac{\partial^2 u}{\partial y^2}\right]+\frac{\mu_r}{\rho_\infty}\frac{\partial \omega}{\partial y}+g\beta_T\left(T-T_\infty\right)cos\varphi-\frac{\sigma B_0^2}{\rho_\infty}u, \tag{2}$$

$$u\frac{\partial \omega}{\partial x}+v\frac{\partial \omega}{\partial y}=\frac{\gamma}{\rho_\infty j}\frac{\partial^2 \omega}{\partial y^2}-\frac{\mu_r}{\rho_\infty j}\left(2\omega+\frac{\partial u}{\partial y}\right), \tag{3}$$

$$u\frac{\partial T}{\partial x}+v\frac{\partial T}{\partial y}=\frac{1}{\rho_\infty c_p}\frac{\partial}{\partial y}\left[\left(\kappa+\frac{16T_\infty^3\sigma^\star}{3k^\star}\right)\frac{\partial T}{\partial y}\right]+\frac{(\mu(T)+\mu_r)}{\rho_\infty c_p}\left(\frac{\partial u}{\partial y}\right)^2+\frac{\sigma B_0^2}{\rho_\infty}u^2. \tag{4}$$

The conditions at the boundary are:

$$\begin{aligned}&u=u_w=cx^r, v=v_w, \omega=-s\frac{\partial u}{\partial y}, -\kappa_\infty\frac{\partial T}{\partial y}=h_f\left(T_f-T\right)\ \ at\ y=0,\\&u\longrightarrow 0, N\longrightarrow 0, T\longrightarrow T_\infty\ \text{ as }\ y\to\infty.\end{aligned} \tag{5}$$

The description of various symbols used in the above equations are hereby given: ω symbolizes microrotation component while u denotes velocity components in x direction whereas v stands for the component of velocity in y direction, μ and μ_r indicate dynamic and vortex viscosity while γ depicts spin gradient viscosity. Furthermore, $\sigma^\star$, ρ_∞, $k^\star$ and j describe Stefan-Boltzmann constant, density

of the ambient fluid, mean absorption coefficient and micro inertial density in that order. Also, T indicates the fluid temperature, T_f describes the surface sheet temperature which is sustained by convection from hot fluid with h_f as the coefficient of heat transfer where $h_f = bx^{(r-1)/2}$ (see [16, 20, 33]) with b being a constant, the ambient fluid temperature is denoted by T_∞, c_p stands for the specific heat at constant pressure whereas κ stands for the thermal conductivity.
The term v_w symbolizes the suction/injection term with $v_w = V_0 x^{(r-1)/2}$, where V_0 is a constant [25, 34] and references there-in), s is a surface boundary parameter with the property $0 \leq s \leq 1$. When $s = 0$ then $\omega = 0$ and this situation describes a strong concentration in which the micro-particles near the wall cannot rotate. A situation of weak concentration of the micro particles is unfolded when $s = 1/2$ and this also relates to the disappearance of anti-symmetric part of the stress tensor whereas $s = 1$ has been found to be applicable for modelling the turbulent boundary layer situations [35-37].
The varying viscosity $\mu(T)$ is expressed as [38-40].

$$\frac{1}{\mu} = \frac{1}{\mu_\infty}\left[1 + \zeta\left(T - T_\infty\right)\right] = H\left(T - T_r\right), \tag{6}$$

where H, μ_∞, T_r and ζ are constants with

$$H = \frac{\zeta}{\mu_\infty}, T_r = T_\infty - \frac{1}{\zeta} \tag{7}$$

and their values are determined by the reference state of the fluid, ζ connotes the thermal nature of the micropolar fluid. Other models of temperature-dependent viscosity includes the Vogel's and the Reynolds viscosity model, however, the model in Eq. (6) has been found to be applicable for a broad range of temperature than the other models [41-42].
The nature of thermal conductivity κ is supposed to vary with temperature in an approximately linear form as

$$\kappa\left(T_f - T_\infty\right) = \kappa_\infty\left[\left(T_f - T_\infty\right) + \delta\left(T - T_\infty\right)\right], \tag{8}$$

where κ_∞ indicates the ambient thermal conductivity, δ stands for the variable thermal conductivity parameter. Meanwhile, [43] reported that the range of values of $0 \leq \delta \leq 6$ is applicable for air while $0 \leq \delta \leq 0.12$ is appropriate for water and $-0.1 \leq \delta \leq 0.12$ for lubrication oils.
By means of Eq. (9) the modelled equations are translated to nonlinear coupled ordinary differential equations [24, 44]

$$\begin{aligned}
&\eta = y\left[\frac{c(r+1)x^r}{2x\nu_\infty}\right]^{1/2},\ \psi = x^{(r-1)/2}\left[\frac{2\nu_\infty c}{(r+1)}\right]^{1/2} f(\eta),\ N = x^{(3r-1)/2}\left[\frac{c^3(r+1)}{2\nu_\infty}\right]^{1/2} g(\eta)\\
&u = cx^r f', v = -\left[\frac{c\nu_\infty(r+1)}{2}\right]^{1/2} x^{(r-1)/2}\left(f + \frac{(r-1)}{(r+1)}\eta f'\right),\ \gamma = \left(\mu + \frac{\mu_r}{2}\right) j,\\
&j = \left(\frac{\nu}{c}\right) x^{(1-r)},\ \theta(\eta) = \frac{T - T_\infty}{T_w - T_\infty} = \frac{T - T_r}{T_w - T_\infty} + \theta r,\ \theta r = \frac{T_r - T_\infty}{T_w - T_\infty}.
\end{aligned} \tag{9}$$

Making use of Eq. (9), then Eq. (6) yields

$$\mu = \left(\frac{\theta r}{\theta r - \theta}\right)\mu_\infty, \tag{10}$$

while Eq. (8) implies

$$\kappa = \kappa_\infty\left(1 + \delta\theta\right), \tag{11}$$

By the use of the stream function described as

$$u = \frac{\partial \psi}{\partial y}, v = -\frac{\partial \psi}{\partial x}, \tag{12}$$

the validity of Eq. (1) holds. Then on substituting Eq. (9) into Eqs. (2-5) and bearing in mind Eqs. (10-11) result to the underlisted Eqs.:

$$\left(\frac{\theta r}{\theta r - \theta} + K\right) f''' + f f'' + K g' - \left(\frac{2r}{r+1}\right) f'^2 - \frac{\theta r}{(\theta r - \theta)^2} \theta' f'' + \left(\frac{2}{r+1}\right) \lambda \theta \cos\varphi - \left(\frac{2}{r+1}\right) M f' = 0, \tag{13}$$

$$(1 + K/2)\, g'' + f g' - \left(\frac{3r-1}{r+1}\right) f' g - \left(\frac{2K}{r+1}\right)(2g + f'') = 0, \tag{14}$$

$$(1 + \delta\theta + Nr)\, \theta'' + \delta \theta'^2 + Pr_\infty f \theta' + \left(\frac{\theta r}{\theta r - \theta} + K\right) Pr_\infty Ec f''^2 + \left(\frac{2}{r+1}\right) Pr_\infty MEc f'^2 = 0. \tag{15}$$

The conditions at the boundary transforms to:

$$\begin{aligned} &\eta = 0 : f' = 1,\ f = fw,\ g = -h f'',\ \theta' = Bi\,(1 - \theta)\,, \\ &\eta \longrightarrow \infty : f' = 0,\ g \longrightarrow 0,\ \theta \longrightarrow 0. \end{aligned} \tag{16}$$

The underlisted symbols denote the nomenclature of the parameters included in Eqs. (13-16)

$$\begin{aligned} &K = \frac{\mu_r}{\mu_\infty},\ M = \frac{\sigma_0 B_o^2}{c\rho_\infty} x^{1-r},\ fw = \frac{-\sqrt{2} V_0}{\left(\sqrt{c\nu(r+1)}\right)},\ \lambda = \frac{Gr_x}{Re_x^2}, \\ &Re_x = \frac{u_w x}{\nu_\infty}, Pr_\infty = \frac{\mu_\infty c_p}{\kappa_\infty},\ Gr = \frac{g\beta_T\,(T_w - T_\infty)\,x}{\nu_\infty^2},\ Ec = \frac{u_w^2}{c_p\,(T_w - T_\infty)}, \\ &\theta r = \frac{-1}{\zeta\,(T_f - T_\infty)},\ Bi = \frac{b}{\kappa_\infty}\sqrt{\frac{2\nu_\infty}{c(r+1)}}. \end{aligned} \tag{17}$$

Where K is the micropolar material parameter, fw is a parameter representing suction/injection and $fw = 0$ describes that the sheet is impermeable, the local magnetic field parameter is symbolized by M. Moreso, λ denotes the buoyancy parameter, Pr_∞ is the ambient Prandtl number while Gr is the Grashof number and the Eckert number is represented by Ec, θr denotes the viscosity variation parameter which is dependent on the temperature difference alongside with the viscosity/temperature nature of the fluid, Bi depicts the Biot number which corresponds to the convective heating and the prime represents differentiation which is done with respect to η.

For the engineering community the skin friction coefficient C_{fx} and the Nusselt number Nu_x are very germane. These quantities are respectively indicated in Eq. (18) where τ_w and q_w symbolize the surface shear stress and heat flux in that order.

$$C_{fx} = \frac{\tau_w}{\rho_\infty u_w^2},\ Nu_x = \frac{x q_w}{\kappa_\infty\,(T_f - T_\infty)}, \tag{18}$$

with

$$\tau_w = \left[(\mu(T) + \mu_r)\frac{\partial u}{\partial y} + \mu_r N\right]_{y=0},\ q_w = -\left[\left(\kappa + \frac{16T_\infty^3\sigma^\star}{3k^\star}\right)\frac{\partial T}{\partial y}\right]_{y=0}, \tag{19}$$

in view of equations (9) and (19), the first part of equation (18) takes the form

$$C_{fx} = \left(\frac{r+1}{2}\right)^{1/2}\left[\frac{\theta r}{\theta r - \theta} + (1-h)\,K\right] Re_x^{-1/2} f''(0), \tag{20}$$

while the second part simplifies to

$$Nu_x = -\,(1+\delta\theta)\,(1+Nr)\left(\frac{r+1}{2}\right)^{1/2} Re_x^{1/2}\theta'(0) \tag{21}$$

Method of Solution

Due to highly nonlinearity of the system of Eqs. (13-15) an analytical solution could not be provided, hence, we have engaged shooting technique in company with order-four Runge-Kutta algorithm to numerically solve the boundary value Eqs. (13-16). In this procedure, a satisfactory finite value of $\eta \to \infty$ has been chosen, say η_∞, this ensures that the numerical solutions satisfy the asymptotic boundary conditions. The nonlinear ordinary differential Eqs. (13-15) are transformed into a system of seven first order simultaneous linear equations by the use of the underlisted quantities.

$$k_1 = f, k_2 = f', k_3 = f'', k_4 = g, k_5 = g', k_6 = \theta, k_7 = \theta', \tag{22}$$

$$k_3' = \frac{-k_1k_3 - Kk_5 + \left(\frac{2r}{r+1}\right)k_2^2 + \frac{\theta r}{(\theta r - k_6)^2}k_7k_3 - \left(\frac{2r}{r+1}\right)\lambda k_6 cos\varphi + \left(\frac{2r}{r+1}\right)Mk_2^2}{\left(\frac{\theta r}{\theta r - k_6} + K\right)}, \tag{23}$$

$$k_5' = \frac{\left(\frac{3r-1}{r+1}\right)f_2f_4 + \left(\frac{2K}{r+1}\right)(2f_4 + f_3) - f_1f_5}{(1 + K/2)}, \tag{24}$$

$$k_7' = \frac{-\delta k_7^2 - Pr_\infty\left[k_1k_7 + \left(\frac{\theta r}{\theta r - k_6} + K\right)Eck_3^2 + \left(\frac{2}{r+1}\right)MEck_2^2\right]}{(1 + \delta k_6 + Nr)}. \tag{25}$$

The boundary condition equations are given as

$$\begin{aligned} &k_1(0) = 0, k_2(0) = 1, k_3(0) = h_1, k_4(0) = -hk_3(0), k_5(0) = h_2, \\ &k_6(0) = 1, k_7(0) = h_3, k_2(\infty) \longrightarrow 0, k_4(\infty) \longrightarrow 0, k_6(\infty) \longrightarrow 0. \end{aligned} \tag{26}$$

Using the shooting technique to systematically determine the unknown initial conditions of h_1, h_2 and h_3 which are corresponding to $f''(0), g'(0)$ and $\theta'(0)$ and are not given. The procedure is carried out repeatedly with a larger value of η_∞ until a solution is gotten for which successive values of $h_1(0), h_2(0)$ and $h_3(0)$ (i.e. the unspecified initial conditions) give a difference after a preferred significant digit. In the present computations, we have found that $\eta_{max} = 10$ with the step sizes $\Delta_\eta = 0.001$ are appropriate to obtain sufficient accuracy with a tolerance level of less than 10^{-8}.

Results Analysis and Discussion

The results obtained in this work have been cross-checked with those obtained in the related studies in the literature for limiting situations so as to evaluate the correctness of the numerical code. Table 1 illustrates the computed values of the skin friction coefficient C_{fx} for variation in the nonlinear stretching parameter r as compared with that of [45] and [32] when $K = \lambda = \varphi = M = fw = 0$ and $\theta r \to \infty$. The comparison emphasizes a good relationship.

Table 1: Comparison of values of C_{f_x} with variations in r

r	[45]	[33]	Present
0.0	0.627547	0.627600	0.627624
0.2	0.766758	0.766900	0.766901
0.5	0.889477	0.889500	0.889602
0.75	0.953786	0.953900	0.954011
1.0	1.000000	1.000000	1.000052
1.5	1.061587	1.061600	1.061649
3.0	1.148588	1.148600	1.148637
10.0	1.234875	1.234900	1.234913
20.0	1.257418	1.257500	1.257436
100.0	1.276768	1.276800	1.276809

To further analyze the results, the reactions of the dimensionless velocity, temperature, microrotation as well as C_{fx} and Nu_x for variations in the main governing parameters have been displayed through various graphs. The computational values of the controlling parameters adopted for plotting various graphs are material(micropolar) $K = 2.0$, viscosity parameter $\theta r = 5.0$, radiation parameter $Nr = 0.2$, buoyancy parameter $\lambda = 0.5$, magnetic field parameter $M = 0.5$, Biot number $Bi = 0.3$, nonlinear parameter $r = 0.5$, angle of inclination $\varphi = \Pi/6$, thermal conductivity parameter $\delta = 0.5$, Ambient Prandtl number $Pr_\infty = 0.73$, suction parameter $fw = 0.2$ and Eckert number $Ec = 0.1$ unless otherwise indicated in the plots.

Figure 2a is a description of the velocity field against η for variation in the material micropolar parameter K in the presence of suction $(fw > 0)$ and injection $(fw < 0)$. It is noticed that the velocity profiles appreciate with a rise in K for both cases. In this figure, is noted also that the thickness of the boundary layer is thinner in the presence of suction than that of injection.

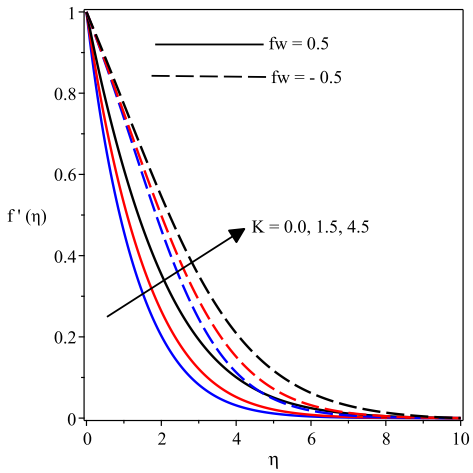

Fig. 2a

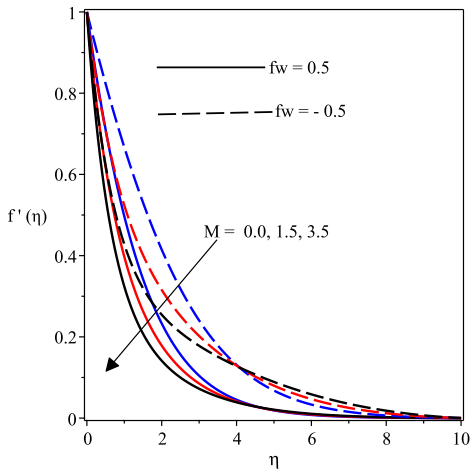

Fig. 2b

Fig. 2: Response of velocity profiles with changes in (a) material parameter K (b) magnetic field parameter M.

Figures 2b reflects the influence of the magnetic field parameter on the velocity profiles for the case of suction and injection. Clearly, the velocity reduces based on the introduction of the Lorentz force which is a resistive force by the applied magnetic field which acts contrary to fluid locomotion. It is noticeable that the thermal and momentum boundary thicknesses are greater for the case of injection than that of suction. The influence of the Eckert number Ec is to boost the velocity distribution as depicted in Figure 3a with a case of injection having a pronounced influence.

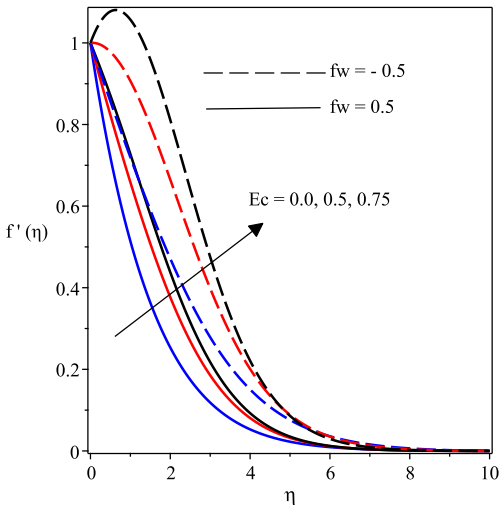

Fig. 3a

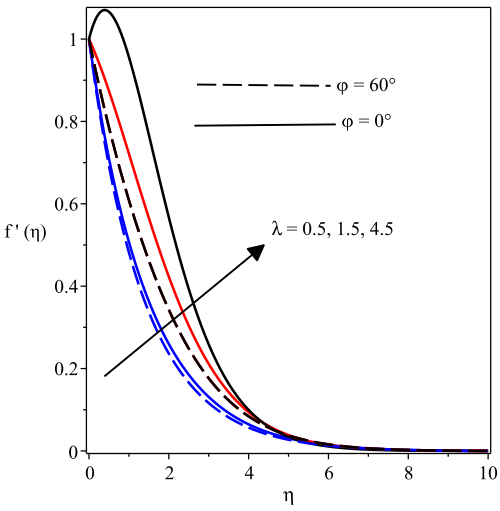

Fig. 3b

Fig. 3: Variations of velocity profiles with (a) Eckert number Ec (b) Buoyancy parameter λ.

Figure 3b depicts the plot velocity field against η for different values of buoyancy parameter λ. Evidently, the velocity increases as the magnitude of λ rises as depicted in Figure 3b. Thus, the motion of the fluid is accelerated by the enhancement in the buoyancy forces corresponding to rising values of λ.

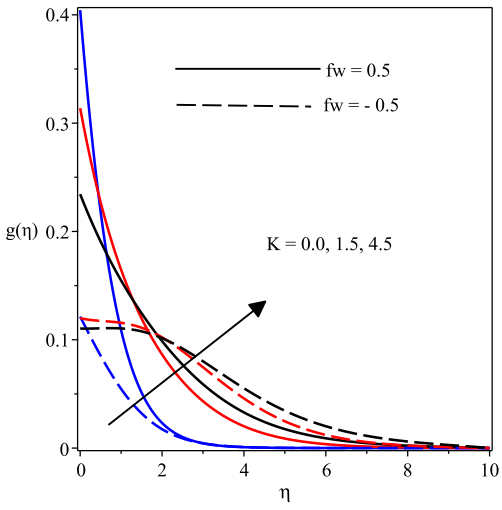

Fig. 4a

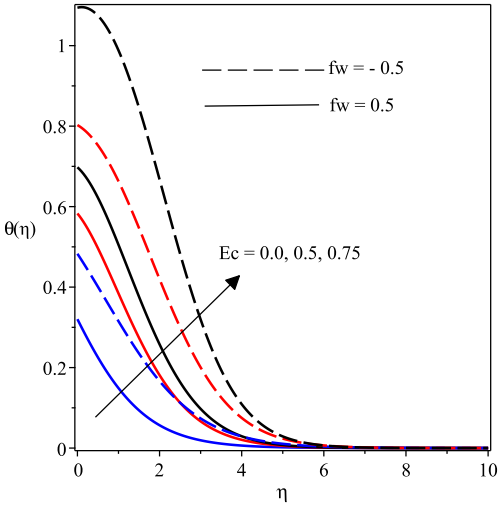

Fig. 4b

Fig. 4: Influence of (a) Material parameter K on microrotation profiles and (b) Eckert number parameter Ec on temperature distribution.

The reaction of microrotation profiles to rising value of K shows that it increases in the presence of both suction and injection parameters as displayed in Figure 4a. Figure 4b shows that the impact of Ec is to boost the temperature due to the friction between the fluid layers. Meanwhile, in consequence of the magnetic field parameter M the temperature distribution is boosted as exhibited in Figure 5a.

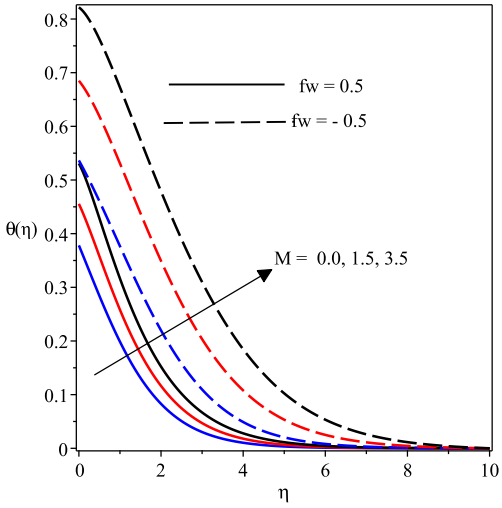

Fig. 5a

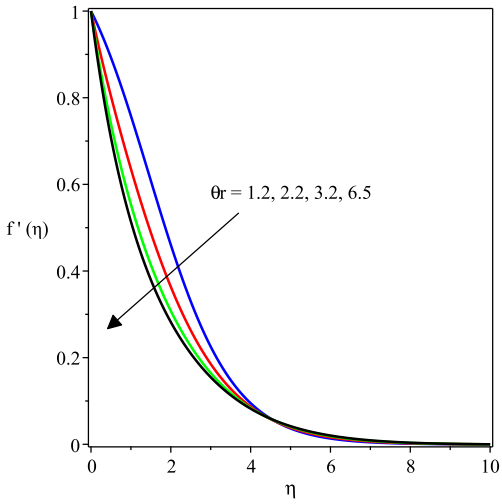

Fig. 5b

Fig. 5: Reactions of (a) temperature distribution to changes in magnetic field parameter M and (b) velocity profiles to variations in viscosity parameter θr.

Figure 6a reveals the response of the velocity field to the changes in the nonlinear stretching parameter r. Here, the effect of r is seen as propelling the thickness of momentum boundary layer to diminish and consequently reduces the locomotion. In the like manner, the microrotation field also falls with growing values of r as seen in Figure 6b.

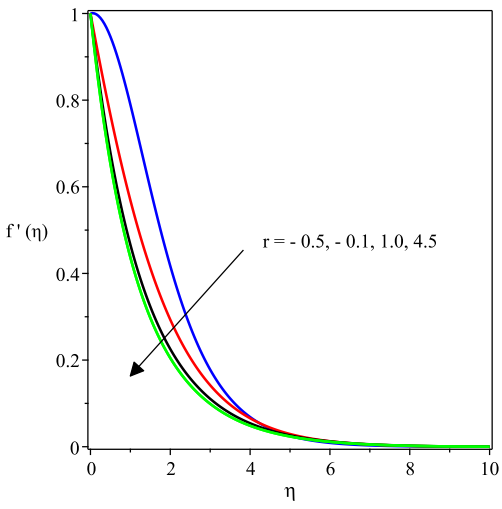

Fig. 6a

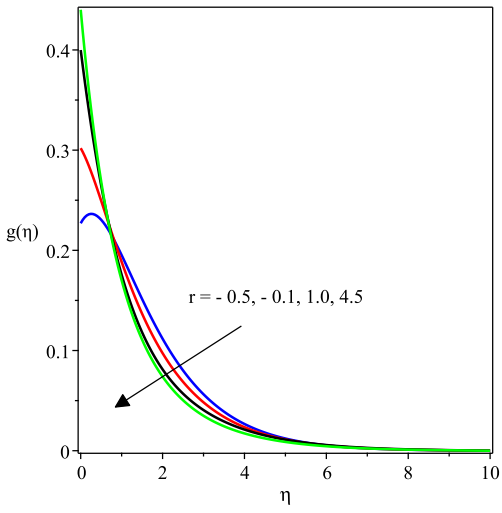

Fig. 6b

Fig. 6: Impact of (a) nonlinear stretching parameter r on velocity field and (b) on microrotation field.

The dimensionless temperature reaction to higher values of the Biot number Bi (indicating the convective heating) in the presence and absence of Ec is displayed in Figure 7a. Clearly, increasing values

of Bi prompts the temperature profile to appreciate. As observed in this figure, the increase is more pronounced in the presence of Ec. In the actual fact, a high Bi is an indication that the internal heat transfer resistance of the sheet is more than that of the surface of the sheet, hence, a rise in the temperature as Bi increases, this observation coincides with that of [32] and [46] for linear surface velocity. Figure 7b exhibits that an increase in δ thickens the thermal boundary layer and aids the growth of temperature distribution and in consequence the rate of heat transfer reduces.

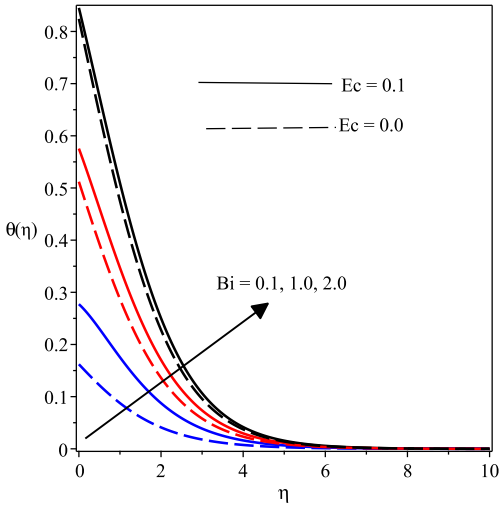

Fig. 7a

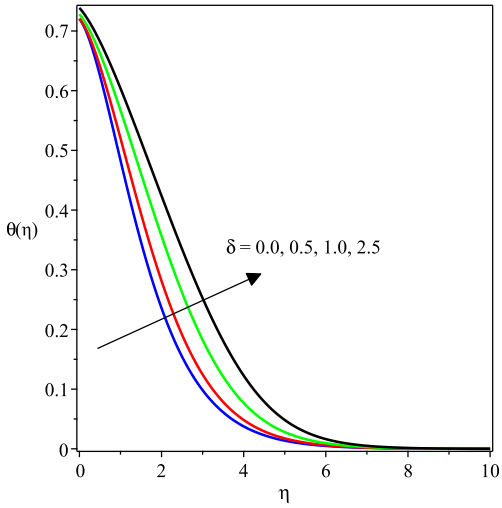

Fig. 7b

Fig. 7: Variations of (a) nonlinear stretching parameter r on velocity field and (b) thermal conductivity parameter δ on temperature distribution.

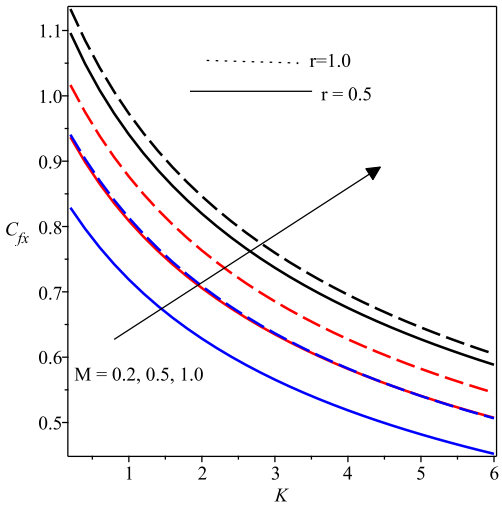

Fig. 8a

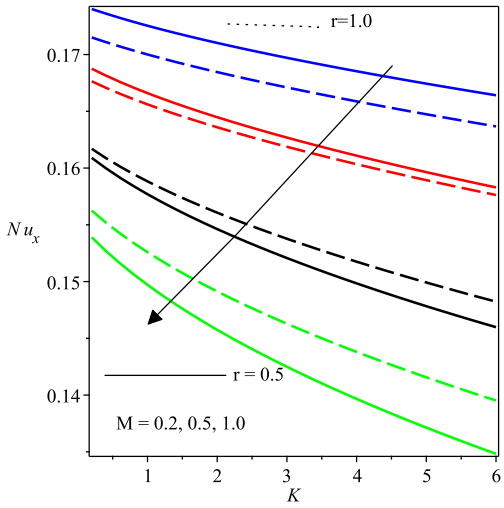

Fig. 8b

Fig. 8: Influences of (a) magnetic field M and micropolar K parameters on C_{fx} (b) magnetic field M and micropolar K parameters on Nu_x.

The combined influences of both material (micropolar) K and magnetic field M parameters on C_{fx} and Nu_x are illustrated in Figures 8a and 8b for $r = 1$ (linear surface velocity) and $r \neq 1$ (nonlinear surface velocity). It is shown that the C_{fx} reduces as K rises whereas the trend reverses with a rise

in M, however, the increase in C_{fx} for a rise in M is more pronounced for a linear stretching case $(r = 1)$ as exhibited in Figure 8a. On the contrary, an increase in K as well as M decelerates Nu_x as revealed in Figure 8b.

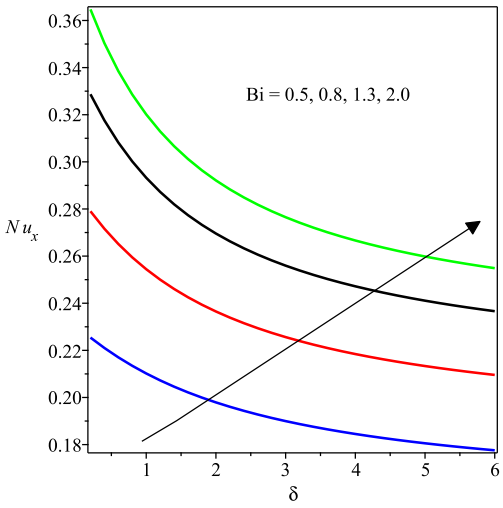

Fig. 9a

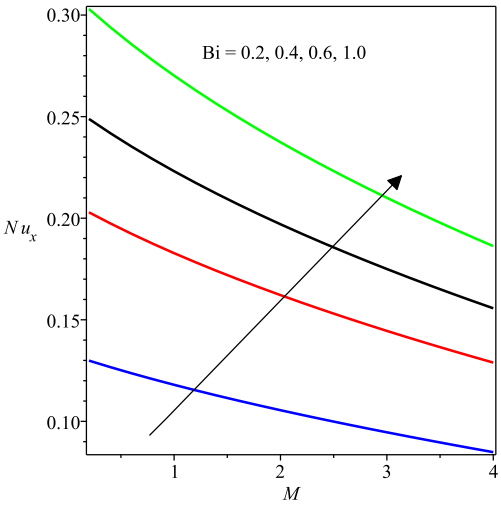

Fig. 9b

Fig. 9: Combined impact of (a) Biot number Bi & thermal conductivity parameters δ on C_{fx} and (b) Bi & M on Nu_x.

The plot of Nu_x versus δ for changes in Bi is depicted in Figure 9a. It is conspicuously seen that an increase in Bi enhances the rate of heat transfer whereas for any fixed value of Bi and an increase in δ, the reverse is the case. Also, Figure 9b reveals a similar pattern to that of Figure 9a for the combined impact of Bi and M on the Nusselt number. The skin friction coefficient C_{fx} is better reduced with a rise in Ec relating to the viscous dissipation in the presence of θr (i.e. variable viscosity) than in its absence $\theta r \to \infty$ (i.e. uniform viscosity) as plotted in Figure 10a.

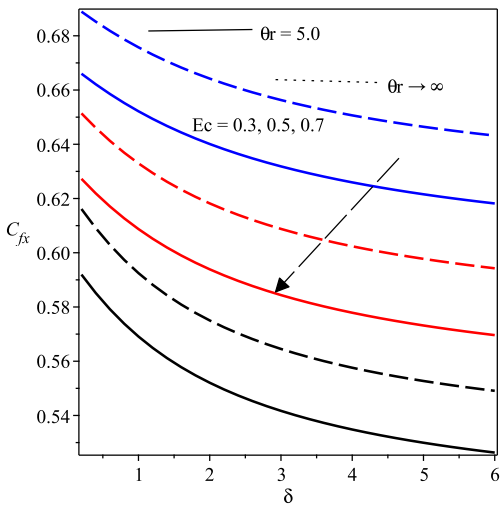

Fig. 10a

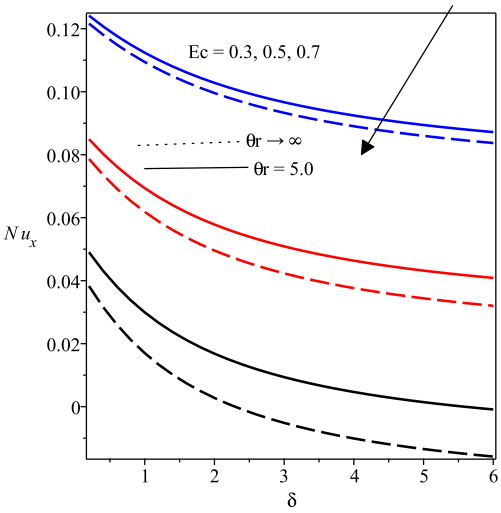

Fig. 10b

Fig. 10: Combined effects of Eckert number Ec & thermal conductivity δ parameters on (a) C_{fx} and (b) Nu_x.

Contrary to the pattern of behaviour in Figure 10a, Nu_x is higher in the presence of θr than when θr is absent with a rise in Ec as illustrated in Figure 10b. It is noticeable that a rise in Ec produces an an increase in the thermal field as stated in Figure 4b whereas it dampens the Nu_x as depicted in Figure 10b, this results coincide with that of [34]. Figures 11a and 11b respectively showcase the combined reaction of Pr and δ on C_{fx} and Nu_x. An increase in Pr enhances both C_{fx} and Nu_x. However, the C_{fx} is better reduced in the presence of θras seen in Figure 11a similarly the heat transfer is better achieved in the presence of $\theta\ r$ as displayed in Figure 11b.

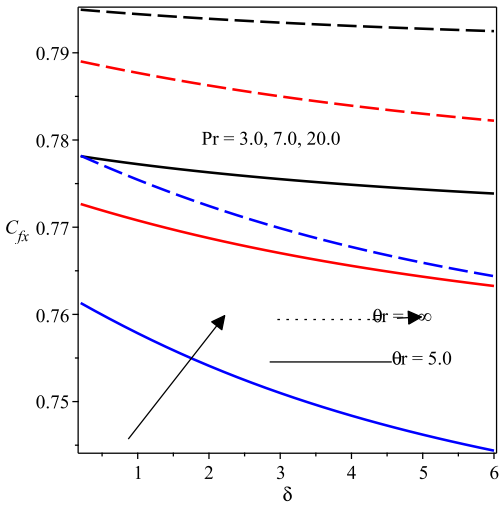

Fig. 11a

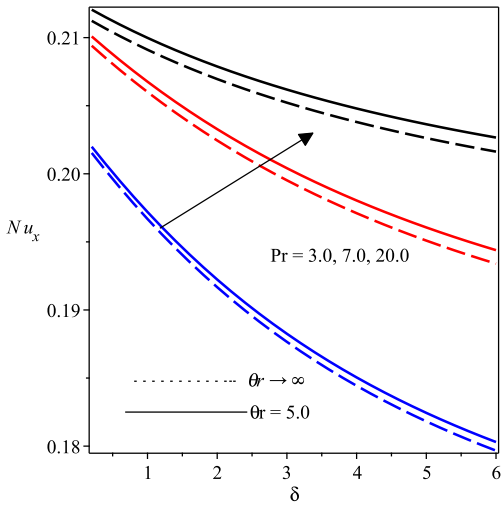

Fig. 11b

Fig. 11: Combined influences of Prandtl number Pr & thermal conductivity parameter δ on (a) C_{fx} (b) Nu_x.

Figure 12a shows the behaviour of C_{fx} for changes in the viscosity parameter θr and in the presence of M. It is noticed that an increases in θr has a rising influence on the C_{fx}. In a similar manner, increasing the inclination angle φ causes the C_{fx} to appreciate with a more prominent influence for a linearly stretching sheet $(r = 1)$ than for nonlinearly stretching sheet as demonstrated in Figure 12b.

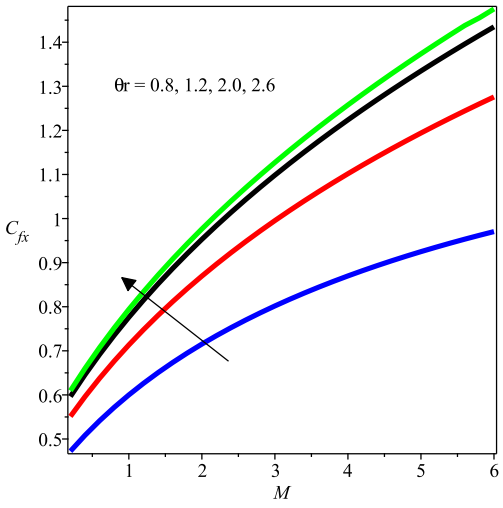

Fig. 12a

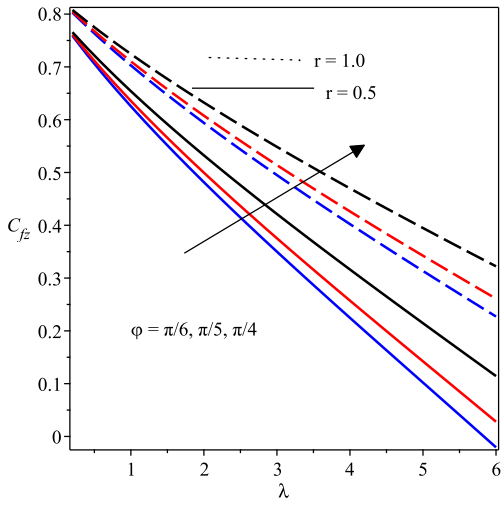

Fig. 12b

Fig. 12: Skin friction coefficient reaction for (a) viscosity θr & magnetic field M parameters and (b) inclination angle φ and buoyancy λ parameters.

Conclusion

This study has numerically analyzed the problem of flow and heat transfer features of hydromagnetic micropolar fluid passing an inclined nonlinearly permeable stretching sheet with variable thermo-physical properties and convective heating at the boundary. The modelled governing equations are converted into dimensionless form by the use of relevant similarity transformations and then solved with shooting technique together with Runge-Kutta algorithm. Summarily, it has been observed that:

- The temperature profiles of the micropolar fluid appreciate by increasing $\theta r, M, \delta, Bi$ and Ec parameters as the microrotation field also thickens with a rise in K.
- The velocity fields of the micropolar fluid accelerate by increasing K, λ and Ec parameters with the momentum boundary layer thickness higher for the case of injection. However, the velocity profiles reduce when the magnitude of $r, \theta r$ and M advance.
- C_{fx} rises with increasing values of $M, \theta r, \varphi$ and Pr whereas the opposite is the case with a rise in K and Ec. An increase Pr and Bi facilitate the transfer of heat but the opposite occurs when the magnitude of K, M and δ advance.

References

[1] M.A. El-Aziz:Journal of the Egyptian Mathematical Society Vol. 21 (2013),385-394.

[2] R.S. Tripathy, G.C. Dash, S.R. Mishra and M.M. Hoque:Engineering Science and Technology, an International Journal Vol. 19 (2016),1573-1581.

[3] A.C. Eringen: J. Math. Anal. Appl. Vol. 16 (1966), 1-18.

[4] A.C. Eringen. Theory of thermo-microfluids, Journal of Mathematical Analysis and Applications. 38 (1972) 480-496.

[5] M. Qasim, I. Khan and S. Shafle: Plos One Vol. 8 (2013) 1-6.

[6] Md. Aurangzaib, S. Uddin, K. Bhattacharyya and S. Shafie: Propulsion and Power (2016) 1-8.

[7] T.S. Kumar, B.R. Kumar, O.D.Makinde and A.G.V. Kumar: Defect and Diffusion Forum Vol. 387 (2018) 78-90.

[8] G. Lukaszewicz. *Micropolar fluids: Theory and Applications* (1st Ed.). Birkhauser, Boston, 1999.

[9] Reena and U. S. Rana: Applications and Applied Mathematics: An International Journal Vol. 4 (2009), 189-217.

[10] O. D. Makinde, G.G. Kumar, S. Manjunatha and B.J. Gireesha:Defect and Diffusion Forum Vol. 378 (2017), 125-136.

[11] B. C. Sakiadis:A.I.Ch.E.J Vol. 7 (1961), 221-225.

[12] L. J. Crane: Communicatios Breves Vol. 21 (1970), 645-647.

[13] N. Afzal: Int. J. Heat Mass Transfer Vol. 36 (1992), 1126-1131.

[14] P.S. Gupta and A.S. Gupta: Can. J. Chem. Eng Vol. 55 (1977), 744-746.

[15] B. K. Dutta and C. Indien: Warme and Stoffubertragung Vol. 23 (1988), 35-37.

[16] A. Ishak: Applied Mathematics and Computation Vol. 217 (2010), 837-842.

[17] E.M.A. Elbashbeshy, D.M. Yassmin and A.A. Dalla: African Journal of Mathematics and Computer Science Research Vol. 3 (2010), 68-75.

[18] O.D. Makinde and W. M. Charles: Appl. Comput. Math Vol. 9 (2010), 243-251.

[19] O.D. Makinde, Z.H. Khan, R. Ahmad and W.A. Khan: Physics of Fluids Vol. 30 (2018), 1-8.

[20] A. Aziz: Commun Nonlinear Simulat. 14 (2010), 1064-1068.

[21] S. Mukhopadhyay: Meccanica Vol. 48 (2013), 1717-1730.

[22] I. Ibrahim and S. M. Suneetha:Int. J. Curr. Res. Aca. Rev Vol. 2 (2014), 89-100.

[23] E. O. Fatunmbi and A. Adeniyan: Journal of Advances in Mathematics and Computer Science Vol. 26 (2018), 1-19.

[24] A.M. Salem:Mathematical Problems in Engineering (2013), 1-10.

[25] K. Das, S. Jana and P.K. Kundu:Alexandria Engineering Journal (2015), 35- 44.

[26] M.S. Tshehla, O.D. Makinde and G.E. Okecha:Research and Essays Vol. 5 (2010), 3730-3741.

[27] A. Postelnicu, T. Grosan and I. Pop:Mech Res Commun Vol. 28 (2001), 331-337.

[28] P.M. Thakur and G. Hazarika:International Journal of Scientific and Innovative Mathematical Research Vol. 2 (2014), 554-566.

[29] S. Jana and K. Das:Italian Journal of Pure and Applied Mathematics Vol. 34 (2015), 20-44.

[30] T.E. Akinbobola and S.S. Okoya:Journal of Nigeria Mathematical Society Vol. 34 (2015),331-342.

[31] E.O. Fatunmbi and O.J. Fenuga:International Journal of Mathematical Analysis and Optimization: Theory and Applications (2017), 211- 232.

[32] M. Waqas, M. Farooq, M.J. Khan, A. Alsaedi, T. Hayat and T. Yasmeen:International Journal of Heat and Mass Transfer Vol. 102 (2016), 766-772.

[33] O.D. Makinde:International Journal of the Physical Sciences Vol. 5 (2010), 700-710.

[34] M.H. Yazdi, S. Abdulaah, I. Hashim and K. Sopian:Energies Vol. 4 (2011), 2273-2294.

[35] G. Ahmadi:Int. J. Engng. Sci. Vol. 14 (1976), 639-646.

[36] S,K. Jena and M.N. Mathur:Int. J. Eng. Sci. Vol. 19 (1981), 1431-1439.

[37] J. Peddieson:Int. J. Eng. Sci. Vol. 10 (1972), 23-32.

[38] K. Kumari: Int. Comm. Heat Mass Transfer Vo. 28 (2001), 723-732.

[39] K.E. Chin, R. Nazar, N.M. Arifin and I. Pop:International Communications in Heat and Mass Transfer Vol. 34 (2007), 464-473.

[40] O.D. Makinde:Entropy Vol. 13 (2011), 1446-1464

[41] D. Knezevic and V. Savic:Facta Universitis Vol. 4 (2006), 27-34.

[42] R. Keimanesh, C. Aghanajafi:Tehniki Vjesnik Vol. 24 (2017), 371-378.

[43] M.A.A. Mahmoud: Physica A. Vol. 375 (2012) 401-410.

[44] T. Hayat, Z. Abbas and T, Javed:Physic Letter A Vol. 372 (2008), 637-647.

[45] R. Cortell:Applied Mathematics and Computation Vol. 184 (2007), 864-873.

[46] M.M. Rahman: Meccanica Vol. 46 (2011), 1127-1143.